Earth and Planetary Science Letters 394 (2014) 94–98

Contents lists available at ScienceDirect

Earth and Planetary Science Letters

www.elsevier.com/locate/epsl

Oxygen escape from the Earth during geomagnetic reversals: Implications to mass extinction

Yong Wei [a,b,c,*], Zuyin Pu [b], Qiugang Zong [b], Weixing Wan [a], Zhipeng Ren [a], Markus Fraenz [c], Eduard Dubinin [c], Feng Tian [d,e], Quanqi Shi [f], Suiyan Fu [b], Minghua Hong [a]

[a] Key Laboratory of Ionospheric Environment, Institute of Geology and Geophysics, Chinese Academy of Sciences, Beituchengxilu #19, 100029, Beijing, China
[b] School of Earth and Space Sciences, Peking University, 100871, Beijing, China
[c] Max-Planck Institute for Solar System Research, 37191, Katlenburg-Lindau, Germany
[d] National Astronomical Observatories, CAS, 100012, Beijing, China
[e] Center for Earth System Sciences, Tsinghua University, 100084, Beijing, China
[f] Shandong Provincial Key Laboratory of Optical Astronomy and Solar-Terrestrial Environment, School of Space Science and Physics, Shandong University at Weihai, 264209, Shandong, China

ARTICLE INFO

Article history:
Received 19 November 2013
Received in revised form 8 February 2014
Accepted 10 March 2014
Available online 1 April 2014
Editor: C. Sotin

Keywords:
atmospheric ion escape
geomagnetic reversal
mass extinction

ABSTRACT

The evolution of life is affected by variations of atmospheric oxygen level and geomagnetic field intensity. Oxygen can escape into interplanetary space as ions after gaining momentum from solar wind, but Earth's strong dipole field reduces the momentum transfer efficiency and the ion outflow rate, except for the time of geomagnetic polarity reversals when the field is significantly weakened in strength and becomes Mars-like in morphology. The newest databases available for the Phanerozoic era illustrate that the reversal rate increased and the atmospheric oxygen level decreased when the marine diversity showed a gradual pattern of mass extinctions lasting millions of years. We propose that accumulated oxygen escape during an interval of increased reversal rate could have led to the catastrophic drop of oxygen level, which is known to be a cause of mass extinction. We simulated the oxygen ion escape rate for the Triassic–Jurassic event, using a modified Martian ion escape model with an input of quiet solar wind inferred from Sun-like stars. The results show that geomagnetic reversal could enhance the oxygen escape rate by 3–4 orders only if the magnetic field was extremely weak, even without consideration of space weather effects. This suggests that our hypothesis could be a possible explanation of a correlation between geomagnetic reversals and mass extinction. Therefore, if this causal relation indeed exists, it should be a "many-to-one" scenario rather the previously considered "one-to-one", and planetary magnetic field should be much more important than previously thought for planetary habitability.

1. Introduction

In the past half a century, many efforts have been devoted to seeking the links between geomagnetic reversals and mass extinctions, but no consensus has been reached (Glassmeier and Vogt, 2010). An important test of any successful mechanism is to explain the patterns of mass extinctions. Fossil records reveal that a mass extinction has a gradual pattern persisting for millions of years, during which a stepwise pattern is manifested by a series of impulsive extinctions (Jin et al., 2000). These patterns suggest that the main cause should be continual environmental degradation. The drop of atmospheric O_2 level has been verified to be able to induce environmental degradation because reducing the supply of O_2 is lethal for most species (Huey and Ward, 2005). However, it is difficult to explain the O_2 level drops if only considering Earth-bounded geochemical processes (Berner, 2005). An alternative possibility is that the O_2 molecules are dissociated into oxygen atoms by solar radiation and subsequently ionized; these O^+ ions are further energized in the ionosphere by the solar wind forcing and can thus overcome the containment by the magnetosphere and gravity, finally escape into the interplanetary space. Since the magnetospheric containment is expected to be severely weakened when the dipole collapses during geomagnetic reversals, we hypothesize that geomagnetic reversals cause O_2 level drops, and the subsequent mass extinctions. To test this hypothesis, in this paper we will examine the newest databases and simulate O^+ escape during reversals.

Fig. 1A shows the newest reversal rate data during the Phanerozoic era (solid line, Ogg et al., 2008). Because of several data gaps

* Corresponding author at Key Laboratory of Ionospheric Environment, Institute of Geology and Geophysics, Chinese Academy of Sciences, Beituchengxilu #19, 100029, Beijing, China. Tel.: +86 10 82998262.
E-mail address: weiy@mail.iggcas.ac.cn (Y. Wei).

http://dx.doi.org/10.1016/j.epsl.2014.03.018

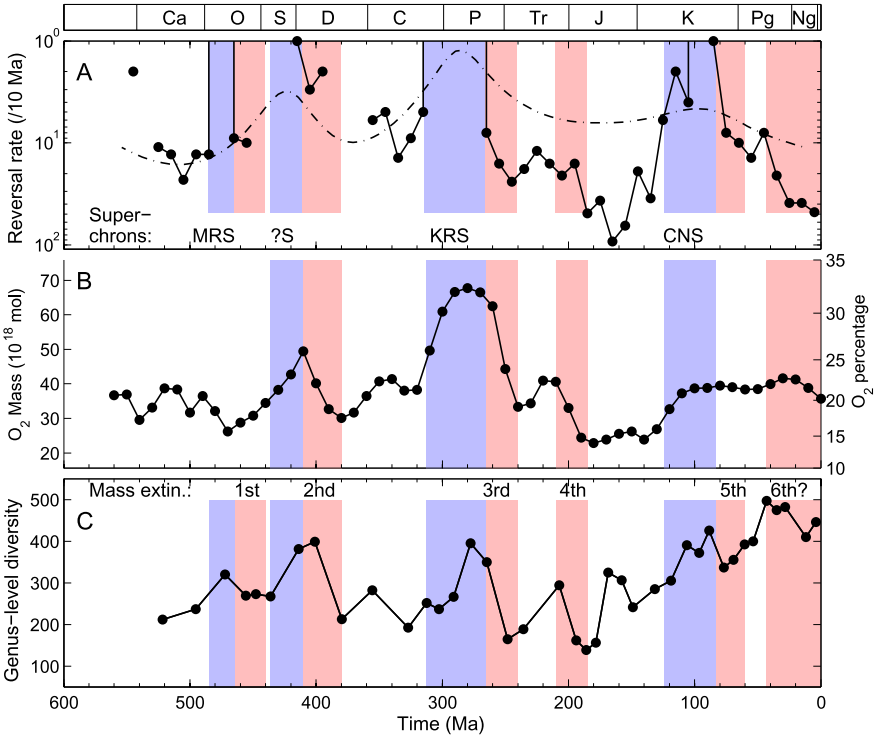

Fig. 1. Temporal evolution of reversal rate, O_2 level and marine diversity over the Phanerozoic era. (A) Geomagnetic reversal rate. The solid line is total reversals within a 10-Myr bin from the new database (Ogg et al., 2008). The dashed line is the relative reversal rate to represent the trend of reversal rate from an older database (McElhinny, 1971). The blue blocks show the superchrons. KRS: Kiaman Reversed Superchron (267–313 Ma). CNS: Cretaceous Normal Superchron (83–125 Ma). MRS: Mayero Reversed Superchron (463–481 Ma). (B) Modeled percentage and amount of atmospheric O_2 over time (Berner, 2009). (C) Number of marine genera (Alroy, 2010). The red blocks show the gradual pattern of 5 well-known mass extinctions, and the 6th mass extinction has not been confirmed. The blue blocks show the superchrons. (For interpretation of the references to color in this figure legend, the reader is referred to the web version of this article.)

in this database, the relative reversal rate from an older database (dashed line, McElhinny, 1971) is also plotted to show the trend of reversal rate for a reference. The reversal rate, atmospheric O_2 level (Fig. 1B) (Berner, 2009) and Marine diversity (Fig. 1C) (Alroy, 2010) show a strong correlation in support of our hypothesis. During the 2nd, 3rd and 4th mass extinctions identified by the diversity drops (red), the reversal rates increased and the O_2 level decreased. On the contrary, when the reversal rate remained at zero or very low, namely during the superchrons (blue) (Merrill and Mcfadden, 1999), the diversity increased, and the O_2 level also increased for 3 out of 4 superchrons. However, during 1st and 5th mass extinction, the reversal rate also increased despite that the O_2 level just remained at low level or had no discernable change. These features suggest that some mass extinctions might be explained by our hypothesis: increasing geomagnetic reversals continually enhance oxygen escape, and this cumulative effect could cause a significant drop of O_2 level over a few millions years. As a result, the global hypoxia might gradually kill numerous species.

2. Explanation and simulation

Planetary ion escape is universal in our solar system throughout its history (Lammer, 2008; Lundin et al., 2007 and Moore and Horwitz, 2007). Many spacecraft observations and theories have revealed that ion escape from terrestrial planets is mainly driven by solar wind dynamic pressure, but the efficiency of this process highly depends on the intensity and morphology of the planetary intrinsic magnetic field (Lundin et al., 2007 and Moore and Horwitz, 2007). Earth's present dipole field interacts with solar wind and forms an intrinsic magnetosphere, and its outer boundary, the magnetopause usually extends to 10 R_E (Earth's radius) at the subsolar point (Fig. 2B). An Earth-like intrinsic magnetic field can effectively prevent the planetary ionosphere from directly interacting with solar wind and thus constrains ion escape (Moore and Horwitz, 2007 and Seki et al., 2001). Mars and Venus have no global intrinsic field, thus their ionospheres directly interact with solar wind and form induced magnetospheres. However, an induced magnetosphere is much smaller in size; for example, Martian magnetopause only extends to 1.2 R_M (Mars' radius) at the subsolar point (Dubinin et al., 2006). Direct comparison of spacecraft observations has illustrated that a Mars-like ion escape is much more efficient in removing planetary O^+ ions (Wei et al., 2012). No doubt, Earth will also have a Mars-like ion escape (Lundin et al., 2007) when Earth's dynamo is substantially weakened (Fig. 2C). Collapse of the dipole during its polarity reversal (Merrill and Mcfadden, 1999) reduces the size of the magnetosphere, thus also causes a transition from the Earth-like ion escape to the Mars-like.

To quantitatively estimate the O^+ escape rate during reversals, we first make an estimate of the evolution of solar wind dynamic pressure (P_{SW}) over Phanerozoic era. Studies of solar analogs suggest that the stellar wind dynamic pressure can be represented as a function of the star's age or X-ray flux (Wood et al., 2002). By using this method the solar wind pressure 600 million years ago (Ma) was 1.3–1.5 times larger than its present value P_{SW0}. Details are given in supplementary material, see Appendix A. If we use X-ray flux, we consider a Sun-like star, 18 Scopii (HD 146233), which is identical to the Sun but ~300 million years (Myr) or more younger than the Sun (Wright et al., 2004). The stellar wind dynamic pressure of 18 Scopii may represent the upper limit of the Phanerozoic P_{SW} because its age overlaps the early Phanerozoic era. This method gives an upper limit of P_{SW} as 3–3.7 times larger than P_{SW0}. Details are given in supplementary material, see Appendix A. The averaged P_{SW0} over one solar cycle is observed as 2–8 nPa, without consideration of space weather effects (Richardson and Wang, 1999). Therefore, the P_{SW} over Phanerozoic era was about 3–30 nPa.

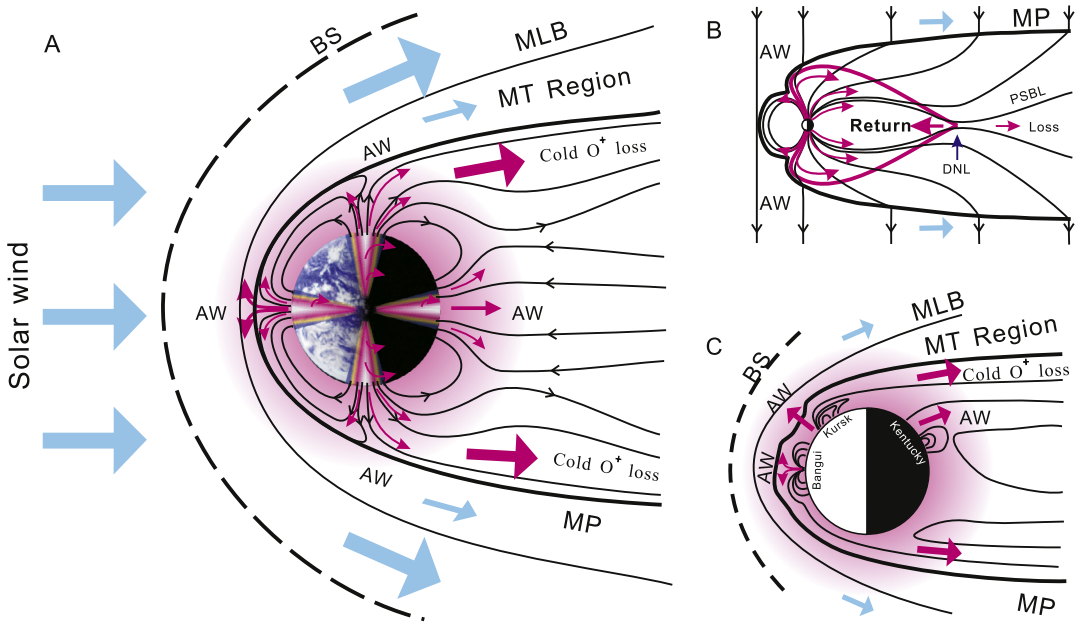

Fig. 2. Ion escape scenarios for the reversing field, present field and no field of Earth. (A) Mars-like ion escape in a quadrupole-dominated magnetosphere for reversing field. This is the view from duskside with two neutral points on the dusk-dawn line. The red region illustrates the O^+ dominated ionosphere, and the four color belts on the Earth denote possible auroral zones. BS: bow shock. AW: auroral wind. MP: magnetopause. MT: momentum transfer. (B) Earth-like ion escape for present field (Moore and Horwitz, 2007): Present Earth's magnetosphere has a Dungey cycle up to 120 R_E tail ward, which can return most of outflowing O^+. DNL: distant neutral line. (C) Fully Mars-like ion escape when the geodynamo totally stops. The magnetosphere is created by the interaction of solar wind with the upper ionosphere, where the crustal field complicates the interaction. (For interpretation of the references to color in this figure legend, the reader is referred to the web version of this article.)

The intensity and morphology of a reversing field are still in debate due to lack of global-scale ancient field records, and they are also probably different from one reversal to another (Merrill and Mcfadden, 1999). Simulations suggest that the total intensity severely decreases; meanwhile, the quadrupole component dominates over the dipole but also decreases by almost one order of magnitude in intensity (Glatzmaier and Roberts, 1995). Following the method proposed by Clement (2004), we construct a reversing field through modifying the present field by reducing the dipole term to zero, multiplying the quadrupole term by 10% and keeping the other terms unchanged. Considering the balance between the Phanerozoic P_{SW} and Earth's magnetic pressure, the averaged position of the magnetopause varies between 1.3 and 1.8 R_E, here we take 1.5 R_E to simplify the calculations. Details are given in supplementary material, see Appendix A. Such a small magnetosphere is morphologically similar to the induced field surrounding Mars, especially concerning the altitude of the magnetopause. Therefore, the ion escape during reversals should be highly Mars-like.

Fig. 2A illustrates the ion escape in the conceptual quadrupole magnetosphere during reversals. The Dungey cycle (Fig. 2B) that returns a substantial fraction of O^+ outflow back to Earth (Nilsson et al., 2013; Moore and Horwitz, 2007 and Seki et al., 2001) does not exist anymore, thus we expect that a major fraction of the O^+ outflow finally escapes. In analogy to the fully Mars-like scenario (Fig. 2C), the ionosphere directly supplies O^+ ions to the near-magnetopause region, where they gain momentum from solar wind and thus are accelerated beyond gravitational escape speed (Lundin et al., 2007 and Dubinin et al., 2006). Moreover, the auroral wind (Moore and Horwitz, 2007) can also deliver O^+ ions to higher altitude by indirectly absorbing solar wind kinetic energy via magnetic reconnection between the magnetic field frozen-in solar wind and the magnetospheric field. The auroral wind might be highly important during space weather events when denser and faster solar wind impacts Earth. The escaping O^+ ions are usually observed over a wide energy range, but most of them are cold and low-energy ions, as observed by many spacecraft for both Earth-like (André and Cully, 2012) and Mars-like escape (Lundin et al., 2008). Here we simply assume that all O^+ ions which have a speed above 10 km/s (the gravitational escape speed near the magnetopause) do escape.

To test the hypothesis, we consider the Triassic–Jurassic event (4th mass extinction) for example. There were 88 reversals within 30 Myr (Ogg et al., 2008), and the O_2 level decreased from 23% to 14% with a total O_2 loss of 15×10^{18} mol (Berner, 2009). Taking an averaged reversing duration of 10^4 yr (Clement, 2004) for each reversal, if the 15×10^{18} mol O_2 escaped into space only during the 88 reversals, the expected O^+ escape rate was about 6.5×10^{29} #/s. In other words, if geomagnetic field reversals could explain the drop of the O_2 level during the Triassic–Jurassic event, the O^+ escape rate should increase to 3 orders of magnitude greater than the present outflow rate of up to 6×10^{26} #/s (Yau and Andre, 1997).

Since we have estimated the P_{SW} and the O^+ escaping speed, the escape rate can be evaluated with a model (Lundin et al., 2007 and Dubinin et al., 2006). The model considers the transfer of momentum from solar wind to ionospheric O^+ ions, and has been successfully applied for the Mars-like ion escape on both Mars and Venus (Lundin et al., 2007 and Dubinin et al., 2006). Therefore, the efficiency of momentum transfer is a critical parameter. The efficiency has been determined as a function of the O^+ density in the momentum transfer region by spacecraft observations on Mars (Perez-de-Tejada, 1998). For the present O_2 level at 21%, the averaged O^+ density in the momentum transfer region is observed to be about 10^4 #/cm^3 (Kitamura et al., 2011). We directly use this value for the O_2 level of 23%, though the expected value should be slightly higher. Considering the classical photochemical reactions (Schunk and Nagy, 2009), the O^+ density is controlled by the ratio of density of O and N_2, and the O density is related to the O_2 density. To simplify the calculations, we assume the O^+ density is linearly related to the ratio of density of O_2 and N_2. When the O_2 level was at 14%, the averaged O^+ density in the momentum transfer region could be about 6×10^3 #/cm^3. According to the relation between the efficiency of momentum transfer and the O^+ density

determined from observations at Mars, the efficiencies at different O_2 level can be estimated. With those parameters derived above, the O^+ escape rate for the reversals during the Triassic–Jurassic event can be simulated. More details are given in supplementary material, see Appendix A.

3. Results and discussion

The results of our simulations (Fig. 3) suggest that O^+ escape driven by a somewhat enhanced solar wind could explain at least 50% of the O_2 drop during the 4th mass extinction. Thus our hypothesis is a possible explanation. The predicted escape rate is much higher than that on present Earth (Moore and Horwitz, 2007), Mars (Lundin et al., 2008) and Venus (Nordström et al., 2013), but comparable with the water loss rate on comet Halley at Earth orbit (Krankowsky et al., 1986), and far less than that on comet Hale–Bopp at Earth orbit (Russo, 2000). The upper limit of O^+ escape rate should be the global production rate of O^+, which is estimated at about 5×10^{30} #/s during solar maximum based on the International Reference Ionosphere (IRI) model (Bilitza et al., 2012). Our escape rate is also below this upper limit. In addition, from Fig. 3 one may note that Earth's present outflow rate is comparable to that of Mars and Venus, and this recently led to a debate on whether a planetary magnetic field can protect a planetary atmosphere (e.g., Barabash, 2010). Wei et al. (2012) have presented observational evidence to support the protective role of the planetary magnetic field. Here our simulations also give an important clue: the Earth's outflow rate should be much higher than Venus and Mars if the Earth's magnetic field is significantly weakened, and the difference is mainly due to the fact that Earth has a higher O^+ density in the interaction region between solar wind and ionosphere.

The uncertainties in this estimate are mainly introduced by poor knowledge of the solar wind dynamic pressure and the intensity of the reversing field in ancient times. However, two other factors, which have not been considered in our simulations, may significantly increase the O^+ escape rate. One is the occurrence of space weather events. The "corotating interaction region" only impacts Mars for 15% of the total time, but can drive at least 33% of the total O^+ escape (Dubinin et al., 2006). The "coronal mass ejection" can even cause 3–7 times higher O^+ loss rates on Mars during high solar activity years than during low solar activity years (Luhmann et al., 2007). Some Sun-like stars younger than our Sun have been observed to be more active (Telleschi et al., 2005), and thus the Sun during Phanerozoic time should produce more frequent space weather events. The other factor is excursion, also called "aborted reversal" (Merrill and Mcfadden, 1999). It occurs more frequently but with shorter duration (several thousand years) than reversals, and could also cause a transition from Earth-like O^+ escape to Mars-like.

There are at least two methods to test our hypothesis. Because ion escape favors the lighter isotopes (Lammer, 2008), severe O^+ escape could have caused an increase of the $^{18}O/^{16}O$ ratio. The other is the stepwise pattern (Jin et al., 2000), of which each step should correspond to one or a series of geomagnetic reversals.

Recently, it has been hotly debated whether we are in the mid of the 6th mass extinction (Barnosky et al., 2011). As shown in Fig. 1, over the last 40 Myr, the reversal rate was increasing and the diversity was decreasing. This implicate that present Earth might be experiencing a new gradual pattern of mass extinction. However, the slight changes of O_2 level cannot be regarded as a strong link between them. More data and work are required to understand these variations.

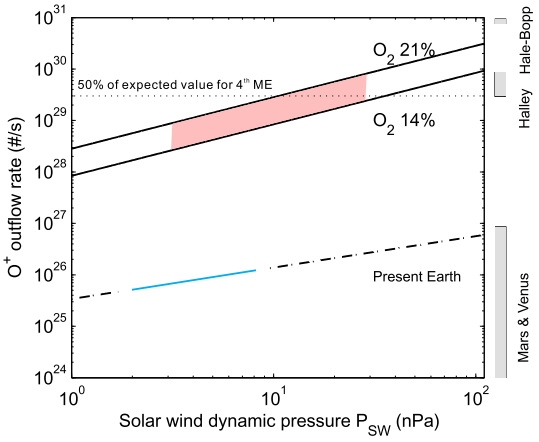

Fig. 3. Simulated O^+ outflow rate under averaged solar wind for O_2 level at 21% and 14%, respectively. The red regions represent Phanerozoic P_{SW}, while the blue segment represents present P_{SW}. The grey bars show the O^+ escape rates of two big comets at the Earth orbit and those of Mars and Venus. (For interpretation of the references to color in this figure legend, the reader is referred to the web version of this article.)

Acknowledgements

We sincerely thank J. Meng, R. Berner and Y. Pan for valuable discussions. This work is supported by Thousand Young Talents Program of China, the National Important Basic Research Project (2011CB811405), Chinese NSFC grant 41321003 and German grant WO910/3-1 within the "Planetary Magnetism" priority program of the Deutsche Forschungsgemeinschaft (DFG) and through grant 50QM0801 of the German Aerospace Agency (DLR).

Appendix A. Supplementary material

Supplementary material related to this article can be found online at http://dx.doi.org/10.1016/j.epsl.2014.03.018.

References

Alroy, J., 2010. The shifting balance of diversity among major marine animal groups. Science 329, 1191–1194.
André, M., Cully, C., 2012. Low-energy ions: a previously hidden solar system particle population. Geophys. Res. Lett. 39, L03101.
Barabash, S., 2010. Venus, Earth, Mars: Comparative ion escape rates. Paper EGU2010-5308 presented at the General Assembly, 2–7 May, Eur. Geosci. Union, Vienna.
Barnosky, A., et al., 2011. Has the Earth's sixth mass extinction already arrived?. Nature 471, 51–57.
Berner, R.A., 2005. The carbon and sulfur cycles and atmospheric oxygen from middle Permian to middle Triassic. Geochim. Cosmochim. Acta 69, 3211–3217.
Berner, R.A., 2009. Phanerozoic atmospheric oxygen: new results using the GEOCARBSULF model. Am. J. Sci. 309, 603–606.
Bilitza, D., et al., 2012. Measurements and IRI model predictions during the recent solar minimum. J. Atmos. Sol.-Terr. Phys. 86, 99. http://dx.doi.org/10.1016/j.jastp.2012.06.010.
Clement, B., 2004. The dependence of geomagnetic polarity reversal durations on site latitude. Nature 428, 637–640.
Dubinin, E., et al., 2006. Plasma morphology at Mars: Aspera-3 observations. Space Sci. Rev. 126, 209–238.
Glassmeier, K.H., Vogt, J., 2010. Magnetic polarity transitions and biospheric effects. Space Sci. Rev. 155, 387–410.
Glatzmaier, G.A., Roberts, P.H., 1995. A three-dimensional self-consistent computer simulation of a geomagnetic field reversal. Nature 377, 203–209.
Huey, R.B., Ward, P.D., 2005. Hypoxia, global warming, and terrestrial late Permian extinctions. Science 308, 398–401.
Jin, Y.G., et al., 2000. Pattern of marine mass extinction near the Permian–Triassic boundary in South China. Science 289, 432–436.
Kitamura, N., et al., 2011. Solar zenith angle dependence of plasma density and temperature in the polar cap ionosphere and low-altitude magnetosphere during geomagnetically quiet periods at solar maximum. J. Geophys. Res. 116, A08227.
Krankowsky, D., et al., 1986. In situ gas and ion measurements at comet Halley. Nature 321, 326–329.

Lammer, H., 2008. Atmospheric escape and evolution of terrestrial planets and satellites. Space Sci. Rev. 139, 399–436.
Luhmann, J., Kasprzak, W., Russell, C., 2007. Space weather at Venus and its potential consequences for atmosphere evolution. J. Geophys. Res. 112, E04S10.
Lundin, R., Lammer, H., Ribas, I., 2007. Planetary magnetic fields and solar forcing: implications for atmospheric evolution. Space Sci. Rev. 129, 245–278.
Lundin, R., et al., 2008. A comet-like escape of ionospheric plasma from Mars. Geophys. Res. Lett. 35, L18203. http://dx.doi.org/10.1029/2008GL034811.
McElhinny, M.W., 1971. Geomagnetic reversals during the Phanerozoic. Science 172, 157–159.
Merrill, R.T., McFadden, P.L., 1999. Geomagnetic polarity transitions. Rev. Geophys. 37, 201–226.
Moore, E., Horwitz, J.L., 2007. Stellar ablation of planetary atmospheres. Rev. Geophys. 45, RG3002.
Nilsson, H., et al., 2013. Hot and cold ion outflow: observations and implications for numerical models. J. Geophys. Res. Space Phys. 118, 105–117. http://dx.doi.org/10.1029/2012JA017975.
Nordström, T., et al., 2013. Venus ion outflow estimates at solar minimum: influence of reference frames and disturbed solar wind conditions. J. Geophys. Res. Space Phys. 118, 3592–3601. http://dx.doi.org/10.1002/jgra.50305.
Ogg, J.G., Ogg, G., Gradstein, F.M., 2008. The Concise Geologic Time Scale. Cambridge Univ. Press, Cambridge, UK.
Perez-de-Tejada, H., 1998. Momentum transport in the solar wind erosion of the Mars ionosphere. J. Geophys. Res. 103, 31499.
Richardson, J., Wang, C., 1999. The global nature of solar cycle variations of the solar wind dynamic pressure. Geophys. Res. Lett. 26, 561–564.
Russo, N., 2000. Water production and release in comet C/1995 O1 Hale–Bopp. Icarus 143, 324–337.
Schunk, R., Nagy, A., 2009. Ionospheres: Physics, Plasma Physics, and Chemistry, second edition. Cambridge Univ. Press, Cambridge.
Seki, K., Elphic, R., Hirahara, M., Terasawa, T., Mukai, T., 2001. On atmospheric loss of oxygen ions from earth through magnetospheric processes. Science 291, 1939–1941.
Telleschi, A., et al., 2005. Coronal evolution of the Sun in time: high-resolution X-ray spectroscopy of solar analogs with different ages. Astrophys. J. 622, 653. http://dx.doi.org/10.1086/428109.
Wei, Y., et al., 2012. Enhanced atmospheric oxygen outflow on Earth and Mars driven by a corotating interaction region. J. Geophys. Res. 117, A03208.
Wood, B., Muller, H., Zank, G., Linsky, J., 2002. Measured mass-loss rates of solar-like stars as a function of age and activity. Astrophys. J. 574, 412–425.
Wright, J., Marcy, G., Butler, R., Vogt, S., 2004. Chromospheric Ca II emission in nearby F, G, K, and M stars. Astrophys. J. Suppl. Ser. 152, 261–295.
Yau, A., Andre, M., 1997. Sources of ion outflow in the high latitude ionosphere. Space Sci. Rev. 80, 1–25.